ON THE APPLICATION OF SIGNAL COMPRESSION USING GOLAY'S CODES SEQUENCES IN ULTRASOUND DIAGNOSTIC

A. NOWICKI, W. SECOMSKI, J. LITNIEWSKI, I. TROTS

Institute of Fundamental Technological Research,
Polish Academy of Sciences
Świętokrzyska 21, 00-049 Warszawa, Poland

P. A. LEWIN

Drexel University, Philadelphia, PA

The issue of maximizing penetration depth with concurrent retaining or enhancement of image resolution constitutes one of the time invariant challenges in ultrasound imaging. Concerns about potential and undesirable side effects set limits on the possibility of overcoming the frequency dependent attenuation effects by increasing peak acoustic amplitudes of the waves probing the tissue. To overcome this limitation a pulse compression technique employing 8 bits Complementary Golay Code (CGS) was implemented at 4 MHz. In comparison with other, earlier proposed, coded excitation schemes, such as chirp, pseudo-random chirp and Barker codes, the CGS allowed virtually side lobe free operation. Computer simulation results for CGS pulse compression are presented. Next, the images of RMI tissue phantom generated by those two excitations schemes are presented. Identical peak power conditions in the experimental setup were implemented with the earlier mentioned 8 bits CGC and 2 periods tone burst. Experimental data indicate that the quality of CGS images is comparable to that acquired using conventional pulse imaging. CGS exhibited signal-to-noise ratio (SNR) gain of 9.6 dB with the axial resolution being virtually the same for both transmitting schemes.

1. Introduction

Maximum range / tissue penetration and fine range resolution which are the two most important considerations in ultrasonographic imaging are contradicting demands.

Sound absorption in the tissue increases approximately linearly with frequency thus limiting the resolution in investigating of the deep structures. On the other hand the possible biological effects related to the insonification limit the probing peak power. The following relationship [2, 5]

$$\frac{\max\ range}{range\ resolution} \leq \frac{burst\ interval}{burst\ width} = \frac{peak\ power}{average\ power}$$

stresses the limit that is imposed by the peak maximum power on the ratio of the penetration depth to the required range resolution.

This limitation can be overcome by using long wide band transmitting sequences and compression techniques on the receiver side [12]. To this end different processing systems were proposed in both, Non Distructive Testing (NDT) and in medical imaging. Basically all use coded transmitted signals and employ correlation and averaging on reception of the echoes. Consequently the high peak transmitted power is no more required – the gain in SNR results from the compression of the echoes. Extensive comparison of the standard radio frequency (r.f.) sine wave bursts compared to the random noise transmission and the subsequent compression using polarity coincidence correlator was done by BILGUTAY *et al.* [2]. They showed the SNR ratio enhancement especially when integration time of the correlator was made arbitrarily long. However the requirements of the real time medical scanning do not permit such extensive integration time and the attained SNR final gain depends on the length of the transmitted sequence and the efficacy of the compression algorithm.

There are several papers in literature concerning similar boundary-condition problem of signal compression in medical diagnostic imaging. COHEN [4] analysed the principles of pulse compressions in radar system concentrating on the behaviour of the linear frequency modulation and binary phase modulation, using Barker, pseudorandom and Golay codes. Suppression of the side lobes after pulse compression was also extensively examined and it was pointed out that using the pulse compression leads to: a) improvement of the detection performance for a given peak power; b) mutual interference reduction; c) increase in system operational flexibility.

The improvement of the SNR in medical ultrasonic imaging was clearly demonstrated by HAIDER *et al.* [7]. The SNR gain was achieved by elongation of the excitation pulse and employment of the deconvolution filter which was implemented as a modified Wiener filter [1] with the deconvolution kernel being the excitation waveform. Authors concentrated on the analysis of the Barker codes of length 7 and 13 and pseudochirp signals. In this case deconvolving with the excitation waveform had several advantages; the excitation waveform was known because it was part of the design and after the deconvolution with the excitation pulse, the resulted compressed echoes had similar waveform characteristics as those, which were obtained with a conventional system. In particular, the range resolution was comparable to that of the pulse system.

Also O'DONNELL [10] showed the penetration improvement in real-time imaging system when using the coded excitation. He used the pulse and the pseudochirp sequence excitation. All measurements were done at center frequency 3.33 MHz and showed the enhanced penetrating power of the coded system comparing to the conventional pulse excitation preserving image quality parameters. Similar results were reported by MISARIDIS *et al.* [9]. In that work the arbitrary function generator was used for the generation of the coded waveforms and the ultrasonic echoes were acquired with 8 bit digital oscilloscope. These experiments were conducted at 4 MHz. When a chirp excitation was applied, the significant reduction in noise level for depths over 10 cm was achieved.

This paper is organized as following. R.f. transmitted ultrasonic signals with phase modulated according to the Barker and Golay binary codes are theoretically simulated and next the experimental in vitro results comparing the echoes from the tissue phantom for burst two period transmission and Complementary Golay Codes at center frequency 4 MHz are demonstrated.

2. The Barker codes

The most widely used binary codes are the Barker sequences. They are optimum in the sense that the autocorrelation function peak is N and the side lobe level falls between $+1$ and -1, where N is the number of subpulses (elements). The compression ratio is proportional to the length of the code, however no Barker code larger than 13 elements has been found. For code length 13 "$+ + + + + - - + + - + - +$" the Peak Side Lobe level. PSL $= 10$ log (maximum side-lobe power / peak response power) is equal to -22.3 dB and Integrated Side Lobe level. ISL $= 10$ log (total power in the side lobes / peak response power) is equal to -11.5 dB. In this work "$+$" refers to a pulse amplitude of "1" or positive phase and "$-$" designates a pulse amplitude of "-1" or negative phase.

Figure 1 compares transmission and matched filtering of a 5 periods sine burst for the uncoded and Barker coded sequence. The total energy in the five periods sequence is five times greater than the one from the single period excitation. After compression
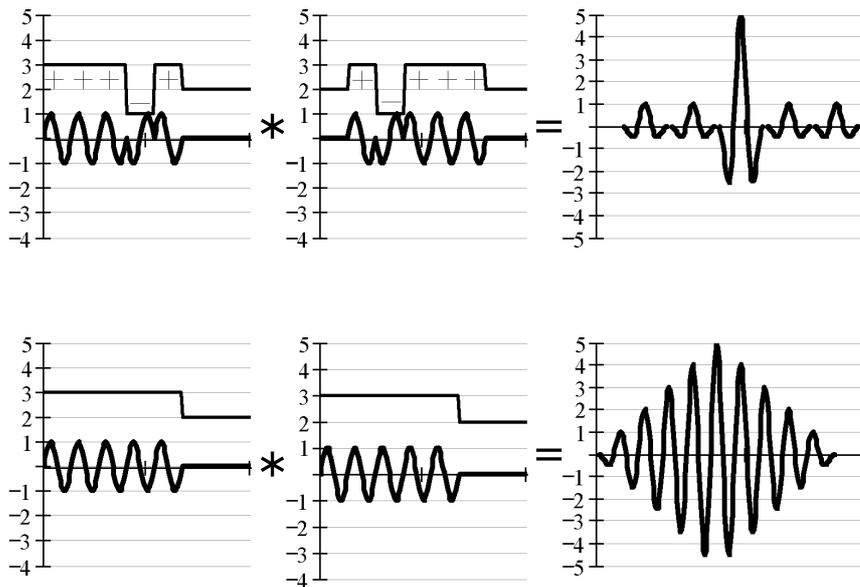

Fig. 1. Comparison of 5 cycles uncoded (bottom) and 5 bits Barker coded – 5 bits (top) pulse sequence and resulting compressed outputs, $\star$ represents convolution operator.

the length of the output is equal to $2N - 1$, 9 in our example, and the peak amplitude is N times greater than the amplitude of the transmitted sequence. Integrated side-lobe level (ISL) increases by 8 dB. The amplitude of the center pulse is five times as large as a single pulse and represents 14 dB SNR improvement for both cases. However, the range lobes for the Barker code case (-14 dB) are much lower than the uncoded case (-2 dB), illustrating the benefit of proper code selection.

In general the range lobe level decreases with code length and much longer code length > 1000 is required for the 60 dB dynamic range of the ultrasonographic images. Barker codes longer than 13 are not known, however there are combined Barker Codes where much larger pulse compression ratio is achievable [4]. Alternatives to matched filtering are mismatched filters [9, 11] minimising side lobes in the least squares sense.

Calculations of two Barker code of length for 7 and 13 bits are shown in Fig. 2. As can be seen the -20 dB width of main lobe is independent on the length of the code and at 4 MHz is equal to 0.4 µs. The amplitude of the compressed signal is proportional to the code length.
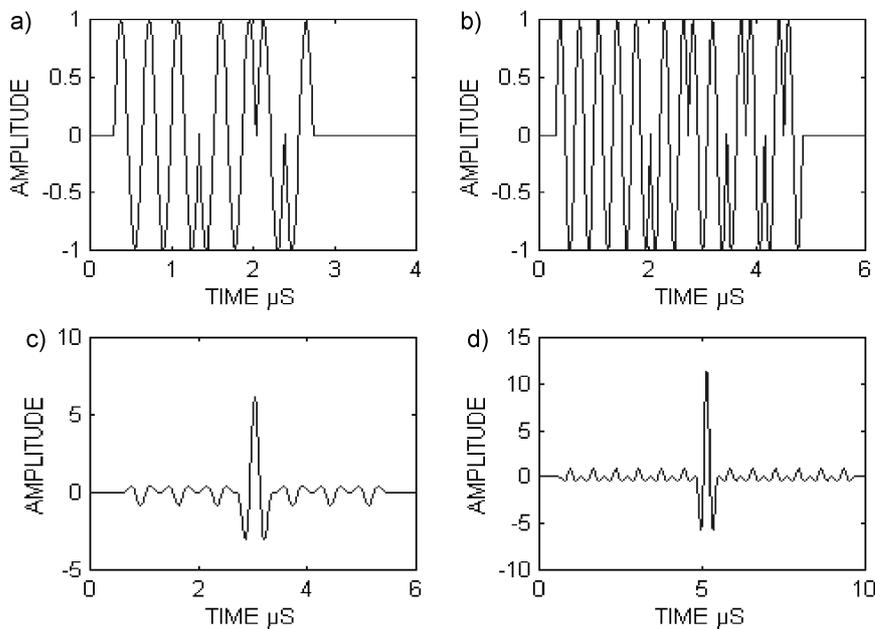

Fig. 2. a) and b) shows sequences of Barker code for 7 and 13 elements respectively; c) and d) shows pulse compression (computer simulation) for 7 and 13 elements respectively for 4 MHz.

3. The Golay codes

The classes of Golay codes are side-lobe-cancelling codes [6] as illustrated in the example in Fig. 3. This property of the Golay codes is as following.
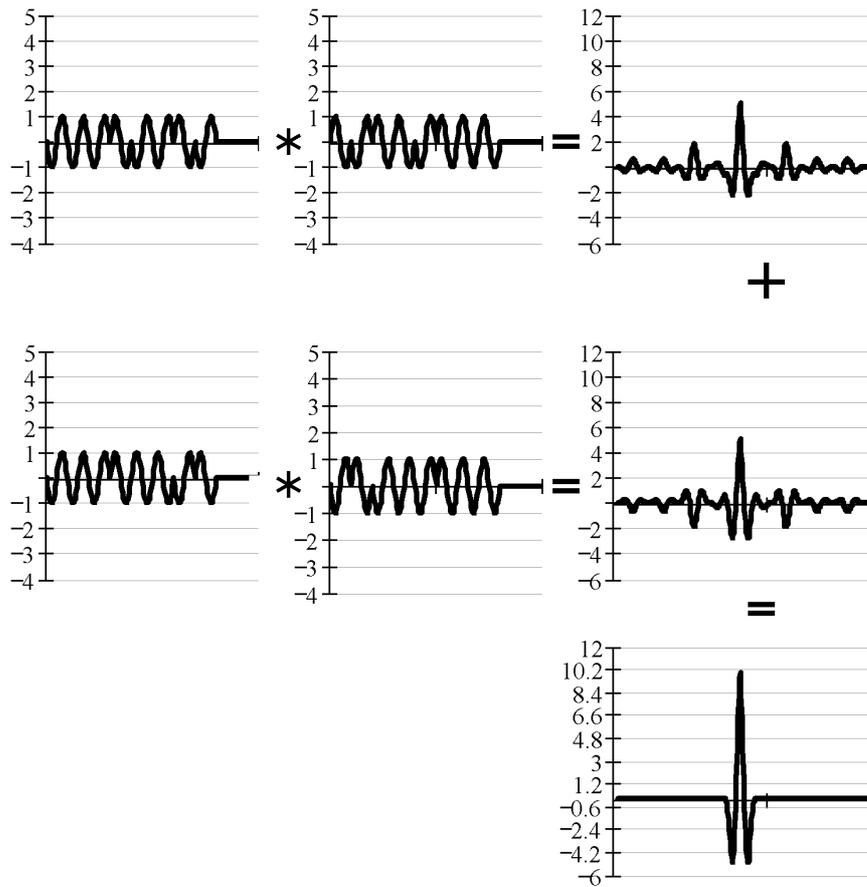
Fig. 3. Principle of side lobe cancellation using pair of Golay complementary sequences of length 8.

Let $\{U_n\}^X$ and $\{U_n\}^Y$ be two discrete phase-coded sequences of length N, consisting of N sine periods with unit amplitude and positive or negative phase. The phase of the Golay pair sequences changes according to the following rule; let X_n and Y_n be a pair of the binary sequences, where X_n and $Y_n \in \{0, 1\}$

$$\{U_n\}^{X,Y} = \{U_0, U_1, \ldots U_{N-1}\}^{X,Y}$$

$$\text{where } X_n \text{ and } Y_n \in \{0, 1\} \tag{1}$$

X and Y are mapped to the new bipolar space $\{+1, -1\}$ according to the rule

$$A_n, B_n = (-1)^{X_n, Y_n}. \tag{2}$$

The n-th element of the sequence as a function of time is given by

$$\{U_n(t)\}^{A,B} = \{U(t - n\tau_p)\}^{A,B} \exp(j\omega t), \tag{3}$$

where τ_p is time duration of the single period of the sine wave with the frequency $\omega = 2\pi f$, $f = 1/\tau_p$.

The aperiodic auto-correlation function of code pair members U^A and U^B of length N is given by expression

$$R^A(\tau) = \sum_{n=0}^{N-1-\tau} \{U_n(t)\}^A \cdot \{U_{n+\tau}(t)\}^A, \qquad \tau \geq 0 \tag{4}$$

and

$$R^B(\tau) = \sum_{n=0}^{N-1-\tau} \{U_n(t)\}^B \cdot \{U_{n+\tau}(t)\}^B, \qquad \tau \geq 0. \tag{5}$$

The property of the Golay complementary series leads to the output peaking at $\tau = 0$ and zeroing otherwise

$$R^A(\tau) + R^B(\tau) = \begin{cases} 2N, & \tau = 0, \\ 0, & \tau \neq 0. \end{cases} \tag{6}$$

The final output is $2N$ times larger than the response to a sine burst. The noise on other hand increases by a factor of $\sqrt{2N}$ and an improvement in SNR is equal $\sqrt{2N}$ in comparison to the single period burst transmission.

Although these codes may seem to represent the ideal solution to the side lobe suppression problem, but in practice tissue and especially blood is moving between the two transmits, so perfect cancellation between the two firings will not be achieved.

Table 1 shows a few codes of Golay. The plus sign refers to a pulse amplitude of "1"; the minus designates a pulse amplitude of "-1".

Table 1. The Golay Codes.

code length	$X(X^*)$	$Y(Y^*)$	Amplitude of the main peak
2	$++(++)$	$+-(-+)$	4
4	$++-+(+-++)$	$+++-(-+++)$	8
8	$+++-++-+$ $(+-++-+++)$	$+++---+-$ $(-+---+++)$	16
16	$--+---+-+++-+--$ $(--+-+++-+----+--)$	$--+----++---+-++$ $(++-+---++----+--)$	32

where X^* and Y^* are code sequences applied for compression using matched filters.

4. Experimental results

The aim of this experiment was to investigate the special features of Golay codes behaviour, their advantages in comparison with ordinary sine-like signal, Barker phased modulated sine sequences and chirp signal. The block diagram of the experimental setup is shown below in the Fig. 4.
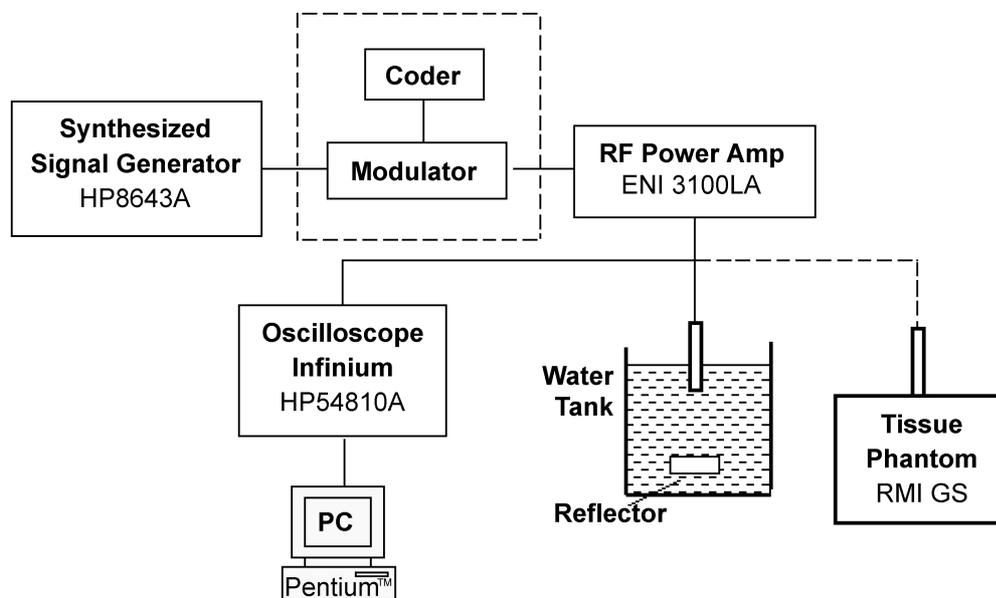

Fig. 4. The experimental setup, for details of the Coder-Modulator block see Fig. 5.

The sinusoidal signals at the frequencies of 4 MHz were synthesised using Signal Synthesiser (HP8643A, Agilent, USA). This signal was connected to the bipolar modulator driven by the {0,1} sequences from the custom design coder, see Fig. 4. The coder preludes programmed logic (EPM7064, Altera$^{\text{TM}}$, USA) allowed to generate one of different transmitter functions: {1,1} sequence resulting in 2 periods of the sine wave and switched pair of 8 bits Golay codes. The prf of the transmitted signals was set to 1 kHz. After amplification in the power rf amplifier (ENI 3100LA, USA) the transmitter burst were exciting the ultrasonic transducer immersed in water tank or moved over the Tissue phantom (Gs, RMI, USA). The excitation voltage applied to the ultrasonic transducer was equal to 50 Vp-p for all different transmitted sequences in order to keep the I_{SPTP} intensity constant (Mechanical Index constant).

The coder (Fig. 5) consists of comparator, PLD logic and analog multiplier. The input signal, sine wave at 0 dBm level, is multiplied either by "1" (output in-phase) or "−1" (output out-of-phase) or "0" (no output signal). The PLD logic is a divide-by-N counter, generating cyclic sequences with pulse repetition frequency and sequence ROM, where different codes are stored.
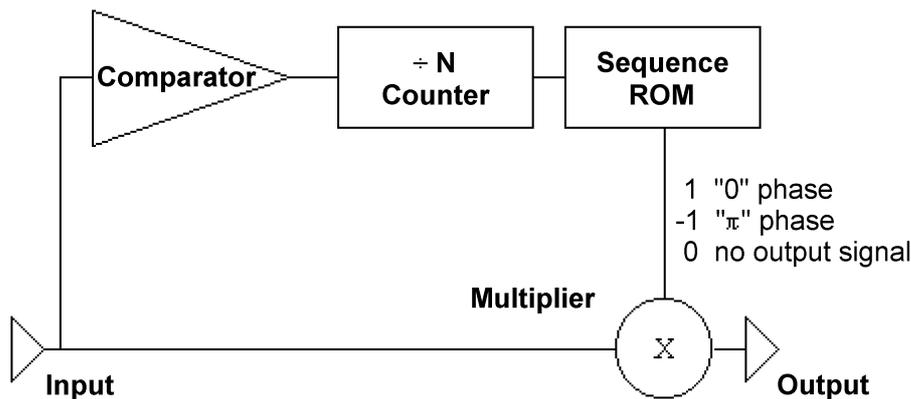
Fig. 5. Block diagram of the custom designed Coder/Modulator circuitry.

The first part of the experiment was to compare the effective overall axial resolution for both transmission modes, namely sine burst and CGS.

Rectangular shape, 2 mm thick perplex sheet acting as a reflector was mounted in the water tank at the axial distance equal to 6 cm. This distance corresponds to the focal distance of the 3.5 MHz transducer used for the experiments.

The RF echoes data were acquired using digital oscilloscope, (see Fig. 4) with a sampling rate 40 ns (25 MHz). Next, the collected digital data were processed off-line and displayed on the oscilloscope. The processing included amplification, pulse compression for Golay sequences, and envelope detection.

Figure 6 shows the RF echoes for two periods sine burst transmission (top), and time compressed complementary Golay series (bottom), respectively. It can be seen that both echoes from the front and rear surface of the perplex reflector are basically identical is shape, however the amplitude of the compressed echoes is approximately 5 times larger than that received from the sine burst transmission. This value is close to the theoretically predicted gain for 8 bits CGS compared to that achievable with the 2 cycles sine burst. Ideally, the expected gain should be 8, however, the finite bandwidth of the pulse-echo transducer slightly elongates the pulse durations and lowers the effective gain.

In Fig. 7 the envelopes of the detected echoes shown in Fig. 6 are depicted. To facilitate the comparison the amplitudes of the envelopes were normalized and it can be seen that their shape is virtually identical. That indicates that rather elaborated reception/compression algorithm for Golay series does not modify or disturb the received signal (here sine burst echoes are considered to be the reference ones).

The next set of experiments was carried out using tissue phantom (GS RMI, Wisconsin, USA) and the results obtained are shown in Fig. 8.

The 3.5 MHz, 6 cm focused transducer was mounted on the xyz micromanipulator's arm and coupled to the phantom through the standard procedure using a thin layer of distilled water.
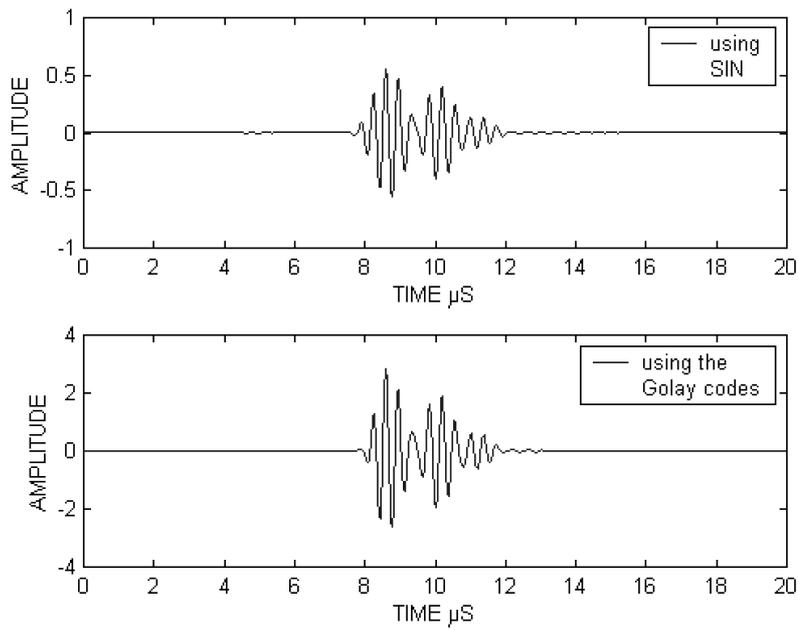
Fig. 6. Echoes from the reflector – plastic sheet, thickness 2 mm. two periods sine burst (top) and Golay codes (bottom).
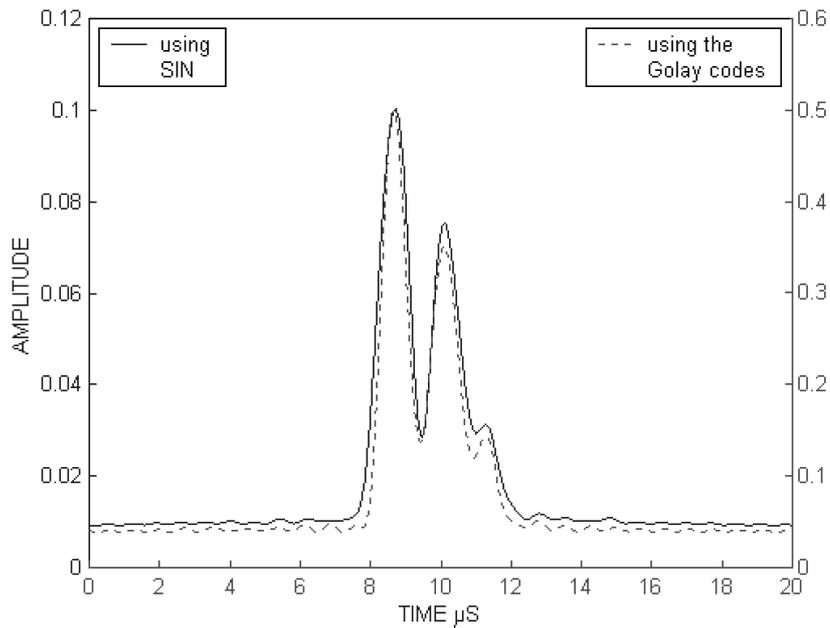
Fig. 7. Comparison of results with using sine-like signal and sequences of Golay codes – envelopes.
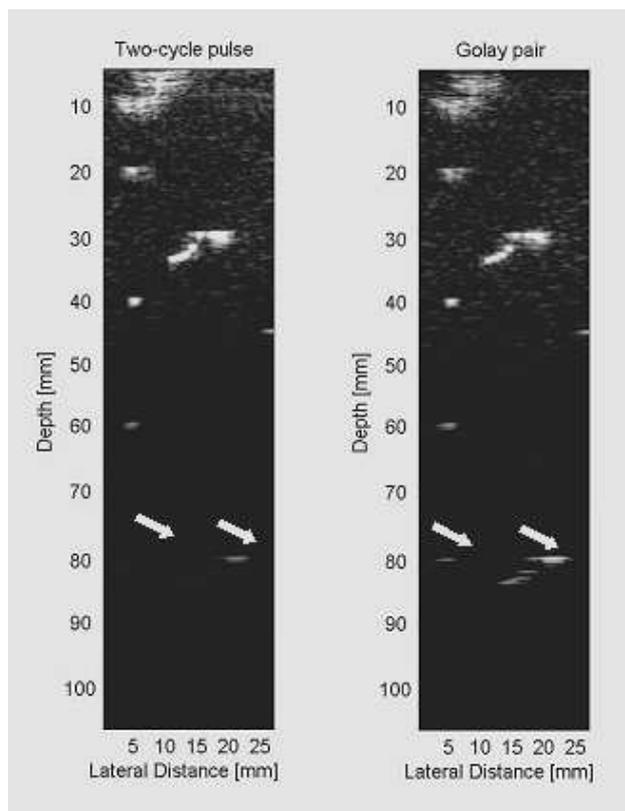
Fig. 8. Ultrasonic images of the Tissue Phantom (GS-RMI, USA) obtained using two periods burst transmission (left) and Complementary Golay Series (right). Arrows show the region of the phantom, where the phantom objects are no more visible for conventional brief pulse excitation and clearly displayed using Golay coded transmission.

The width of the scan shown in Fig. 8 corresponds to 25 mm. Fifty scan lines for each transmission modes were acquired in 0.5 mm intervals. The echoes were processed accordingly, that is as noted above, the CGS required pulse compression, in addition to amplification and envelope detection. Next, the processed signals were displayed in the B-mode linear array format.

The left hand side of Fig. 8 corresponds to the image obtained using sine burst transmission and the right hand side shows an image generated using Complementary Golay Series (CGS).

The improved quality of the CGS image is noticeable. As discussed previously, this image exhibits the gain of 9.6 dB in signal-to-noise ratio in comparison to that produced by the sine burst transmission. The noise present in the sine burst image is clearly suppressed in the CGS one, indicating considerable improvement in dynamic contrast.

5. Conclusions

Increasing tissue penetration preserving fine range resolution is rather contradicting demands in standard ultrasonography. Ultrasonic energy absorption in tissue increases with frequency prohibiting sending higher frequency pulses when examining the deep structures. Possible biological effects limit the peak transmitted power. One way of enlarging the penetration is then increasing the average power by elongation of the transmitted signals with the predetermined signature – code.

Pulse compression of Golay complementary echoes sequences has been described and it was proved to improve almost three times SNR of the ultrasonographic images in comaparison to the standard ultrasonography driven with the sine short burst excitation.

Authors implemented the inherently side lobes free paired transmission of the complementary series (8 bit each) called Golay Codes. The computer simulation results proved the theoretical behavior of the Golay Code Compression (GC) and its advantageous over the standard two period pulse echo system. The experimental studies of reconstructed images obtained from the Tissue Phantom RMI GS showed excellent penetration down to 15 cm without sacrificing the axial resolution and contrast resolution. Even the shallow structures are more clearly visualized with improved contrast resolution, thanks to removal off the spurious clutter reflections. The future work will include the development and implementation of custom design DSP echo compressor allowing the real time imaging.

Acknowledgment

References

[1] J. BIEMOND, R. L. LAGENDIJK, R. M. MERSEREAU, *Iterative methods for image deblurring*, Proc. IEEE, **78**, 856–883, May 1990.

[2] N.M. BILGUTAY, E.S. FURGASON, V. L. NEWHOUSE, *Evaluation of the random signal correlation system for ultrasonic flaw detection*, IEEE Trans. Sonics and Ultrasonics, **SU-23**, 5 (1976).

[3] R. Y. CHIAO, L. Y. MO, A. L. HALL, S. C. MILLER, *B-Mode blood flow imaging*, IEEE Int. Ultra. Symp., Puerto Rico, October 22–25, 2000.

[4] N. COHEN MARVIN, *Pulse compression in pulse-Doppler radar systems*, [in:] Airborn pulsed Doppler radar, G. MORRIS, L. HARKNESS [Eds.], Ch. 9, 173–214, Artech House, Boston 1996.

[5] E.S. FURGASON, V.L. NEWHOUSE, N.M. BILGUTAY, G.R. COOPER, *Application of random signal correlation techniques to ultrasonic flow detection*, Ultrasonic, **13**, 11–17 (1975).

[6] M. J. E. GOLAY, *Complementary series*, IRE Trans. Inf. Theory, **IT-7**, 82–87 (1961).

[7] B. HAIDER, P. A. LEWIN, K. E. THOMENIUS, *Pulse elongation and deconvolution filtering for medical ultrasonic imaging*, IEEE Trans. Ultrason. Ferroelectr. Freq., **45**, 98–113, January 1988.

[8] B.B. LEE, E.S. FURGASON, *High speed digital Golay code flawdetection system*, Ultrasonic, **21**, 153–161 (1983).

[9] T.X. MISARIDIS, K. KIM GAMMELMARK, CH. H. JORGENSEN, N. LINDBERG, A.H THOMSEN, M. H. PEDERSEN, J.A. JENSEN, *Potential of coded excitation in medical ultrasound imaging*, Ultrasonics, **38**, 183–189 (2000).

[10] G. V. MORRIS, *Airborne pulsed Doppler radar*, Artech House, Ch. 8, 1988.

[11] M. O'DONNELL, *Coded excitation system for improving the penetration of real-time phased-array imaging systems*, IEEE Trans. Ultrason. Ferroelectr. Freq. Cont., **UFFC-39**, 341–351, May 1992.

[12] E. A. ROBINSON, S. TREITEL, *Geophysical signal analysis*, Englewood Cliffs: Prentice-Hall, 1980.

[13] M.I. SKOLNIK, *Introduction to radar system*, McGraw-Hill, USA 1962.